Cell Reports, Volume *24*

Supplemental Information

Crosstalk between PKCα and PI3K/AKT Signaling Is Tumor Suppressive in the Endometrium

Alice H. Hsu, Michelle A. Lum, Kang-Sup Shim, Peter J. Frederick, Carl D. Morrison, Baojiang Chen, Subodh M. Lele, Yuri M. Sheinin, Takiko Daikoku, Sudhansu K. Dey, Gustavo Leone, Adrian R. Black, and Jennifer D. Black

Figure S1 Hsu et al.

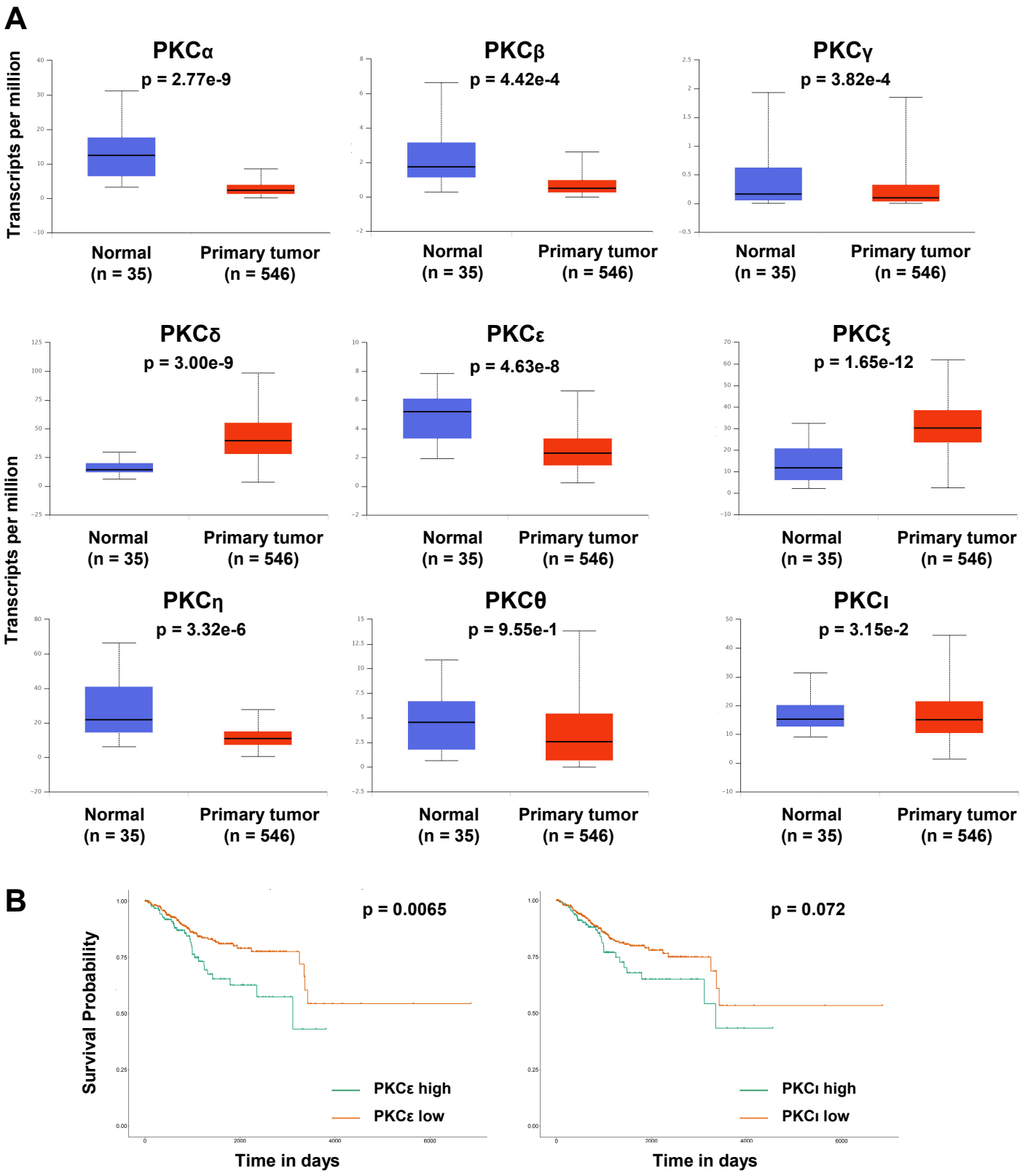

Figure S1. PKC isozyme mRNA expression profiles and correlation with survival probability in EC (related to Figure 1). (A) PKC isozyme mRNA levels in normal endometrium vs primary endometrial tumors. While PKCα, β, ε, and η mRNA expression is reduced in ECs, levels of PKC δ and ζ mRNA are increased, and PKCγ, θ and ι mRNA expression is essentially unchanged in these tumors. (B) Correlation between PKCε or PKCι expression and survival probability. High levels of either PKCε or ι are associated with reduced survival in EC patients, consistent with the identification of tumor promoting functions of PKCε and ι in other cancer types (see text). Results were obtained from analysis of TCGA data.

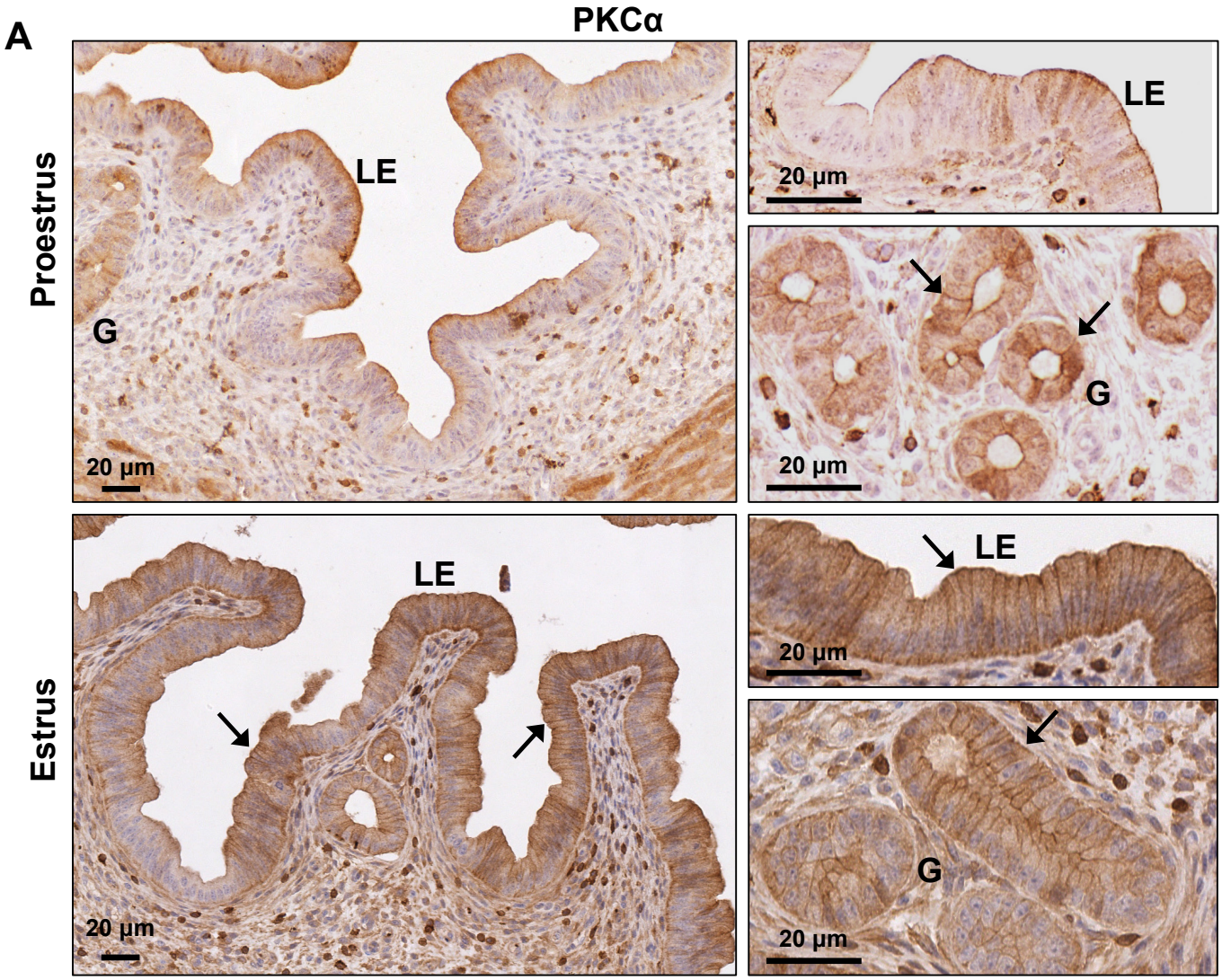

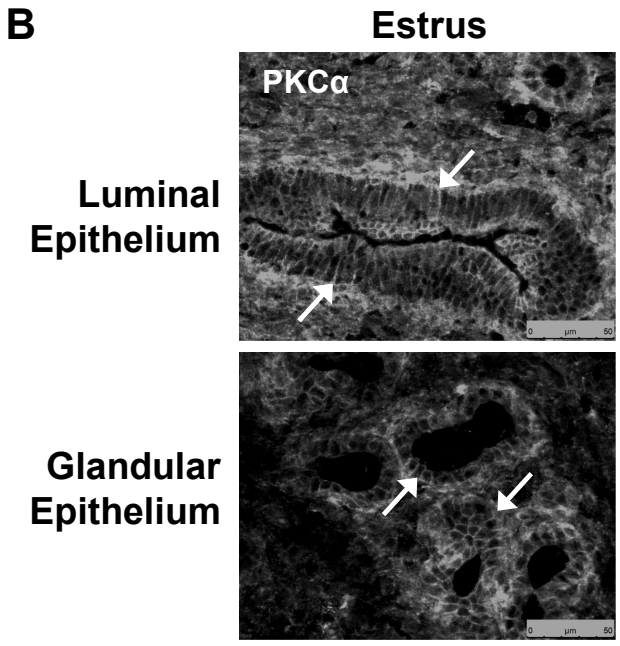

Figure S2. Expression and subcellular distribution of PKCα in the mouse endometrium during proestrus and estrus phases (related to Figure 2).
(A) IHC analysis of PKCα expression in the luminal (LE) and glandular (G) epithelial compartments of uterine tissue during late proestrus and estrus. Membrane-associated localization of PKCα indicates activation of the kinase. In late proestrus, PKCα expression is cytoplasmic in the luminal compartment but membrane-associated in the glands (arrows). In estrus, membrane association of PKCα is detected in both the luminal and glandular epithelium (arrows).
(B) Immunofluorescence staining for PKCα in frozen sections of luminal and glandular epithelium in estrus phase, confirming the localization seen in paraffin sections.

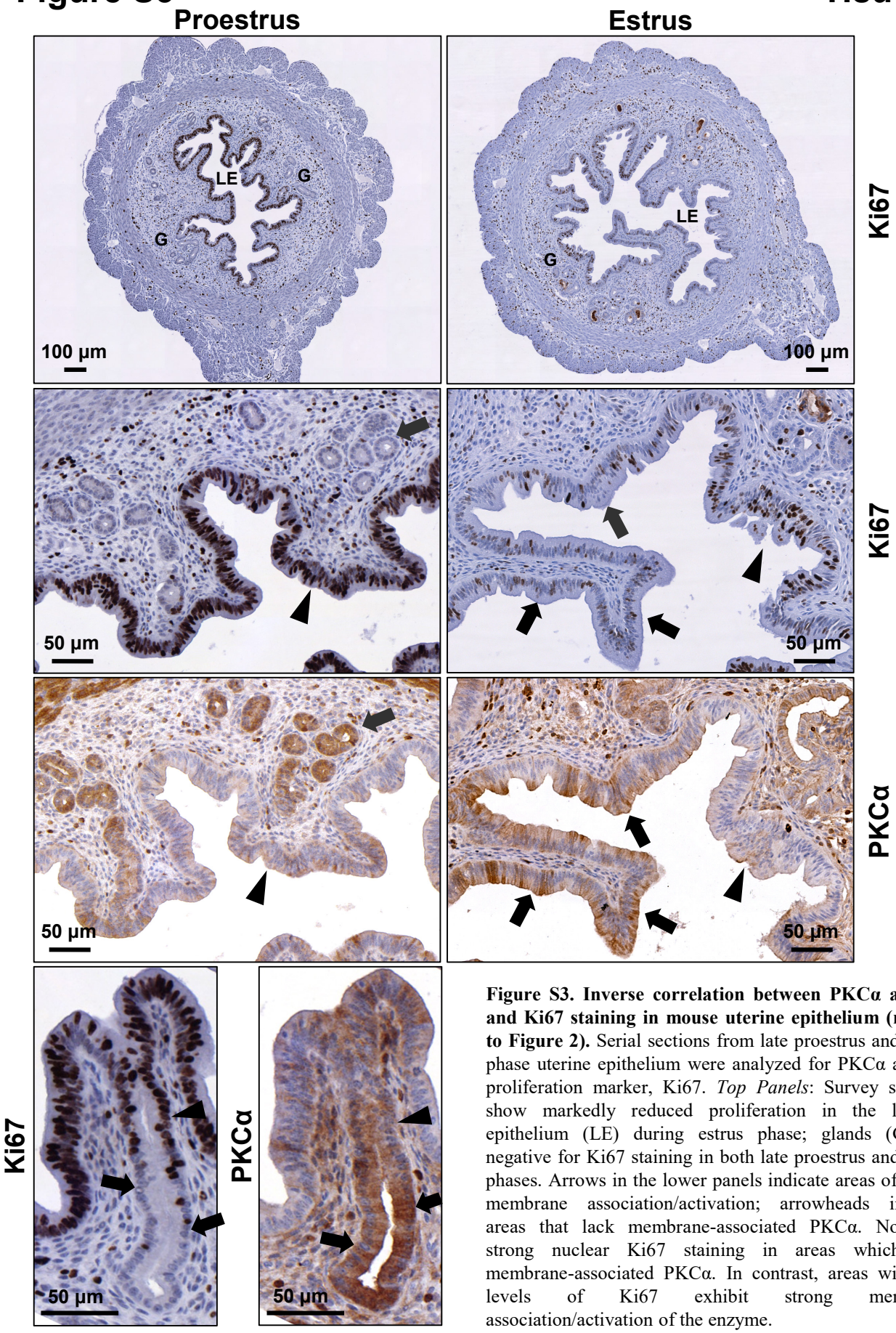

Figure S3. Inverse correlation between PKCα activity and Ki67 staining in mouse uterine epithelium (related to Figure 2). Serial sections from late proestrus and estrus phase uterine epithelium were analyzed for PKCα and the proliferation marker, Ki67. *Top Panels*: Survey sections show markedly reduced proliferation in the luminal epithelium (LE) during estrus phase; glands (G) are negative for Ki67 staining in both late proestrus and estrus phases. Arrows in the lower panels indicate areas of PKCα membrane association/activation; arrowheads indicate areas that lack membrane-associated PKCα. Note the strong nuclear Ki67 staining in areas which lack membrane-associated PKCα. In contrast, areas with low levels of Ki67 exhibit strong membrane association/activation of the enzyme.

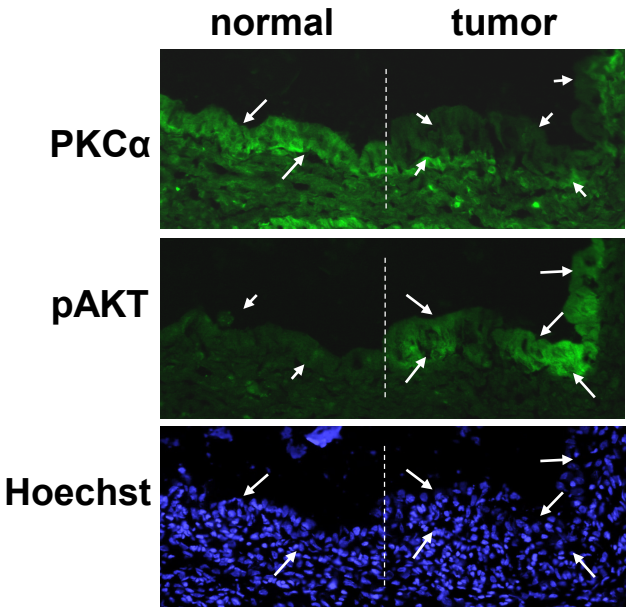

Figure S4. Laser capture microdissection of uterine epithelium guided by immunofluorescence staining for PKCα or pAKT S473 (related to Figure 2). Immunofluorescence analysis of serial sections of frozen uterine tissue from a 9 month *Pten*$^{\Delta 4\text{-}5/+}$;*Prkca*$^{+/+}$ mouse identifies normal epithelium (PKCα^{pos}; pAKT^{neg}) and tumor lesions (PKCα^{neg}; pAKT^{pos}). The presence of PKCα or pAKT is indicated by larger arrows; small arrows identify regions that are negative for marker expression. PKCα mRNA expression in normal and tumor tissue isolated by laser microdissection was quantified by qRT-PCR analysis and results are shown in Figure 2E.

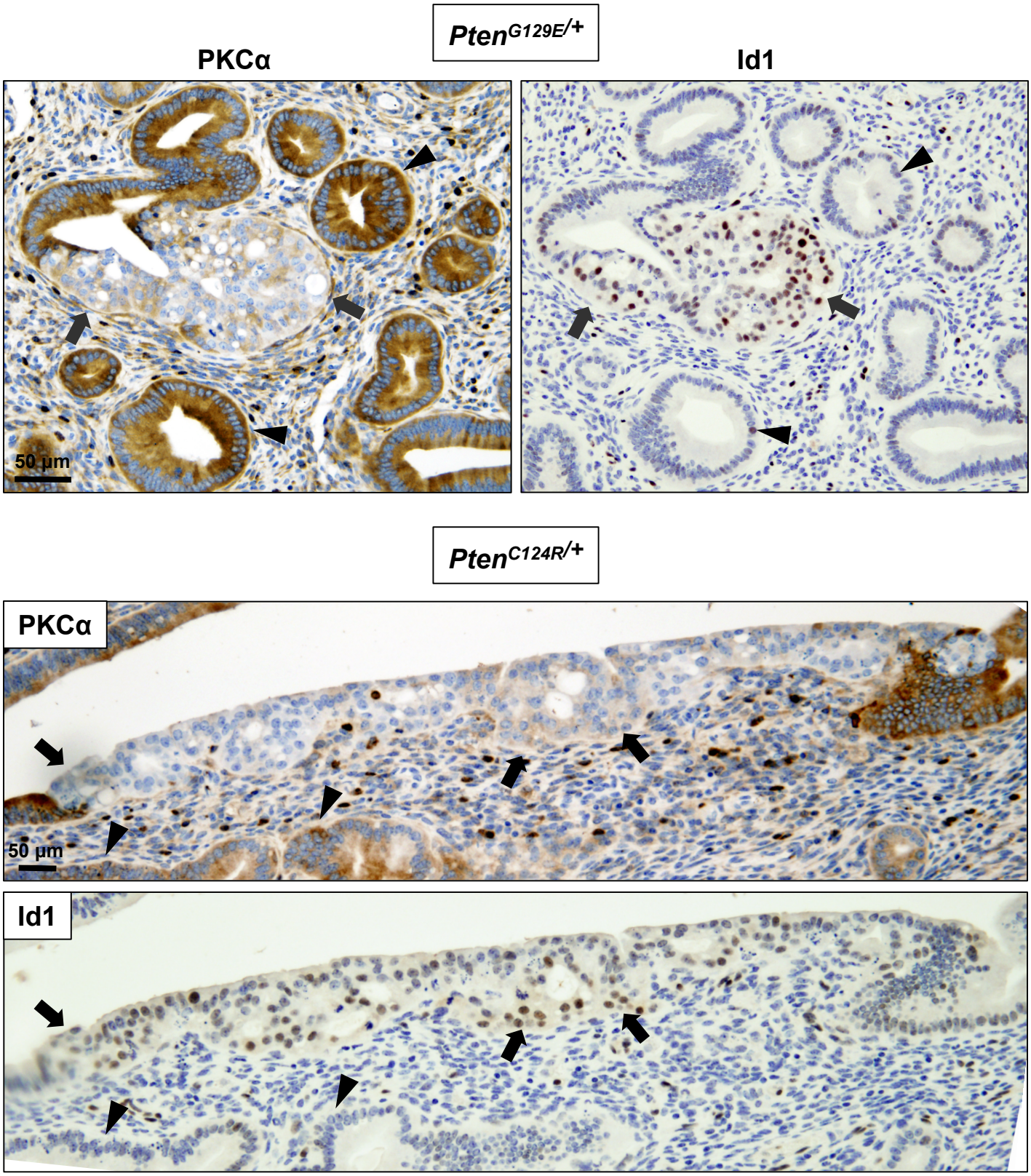

Figure S5. Enhanced Id-1 expression in endometrial hyperplasia correlates with loss of PKCα (related to Figures 2 and 5). IHC analysis of PKCα and Id1 expression in endometrium from *Pten*$^{G129E/+}$ and *Pten*$^{C124R/+}$ mice. Note the strong nuclear staining for Id-1 in hyperplastic regions that lack PKCα (arrows). Arrowheads indicate normal endometrial glands with high PKCα and low Id1 expression.

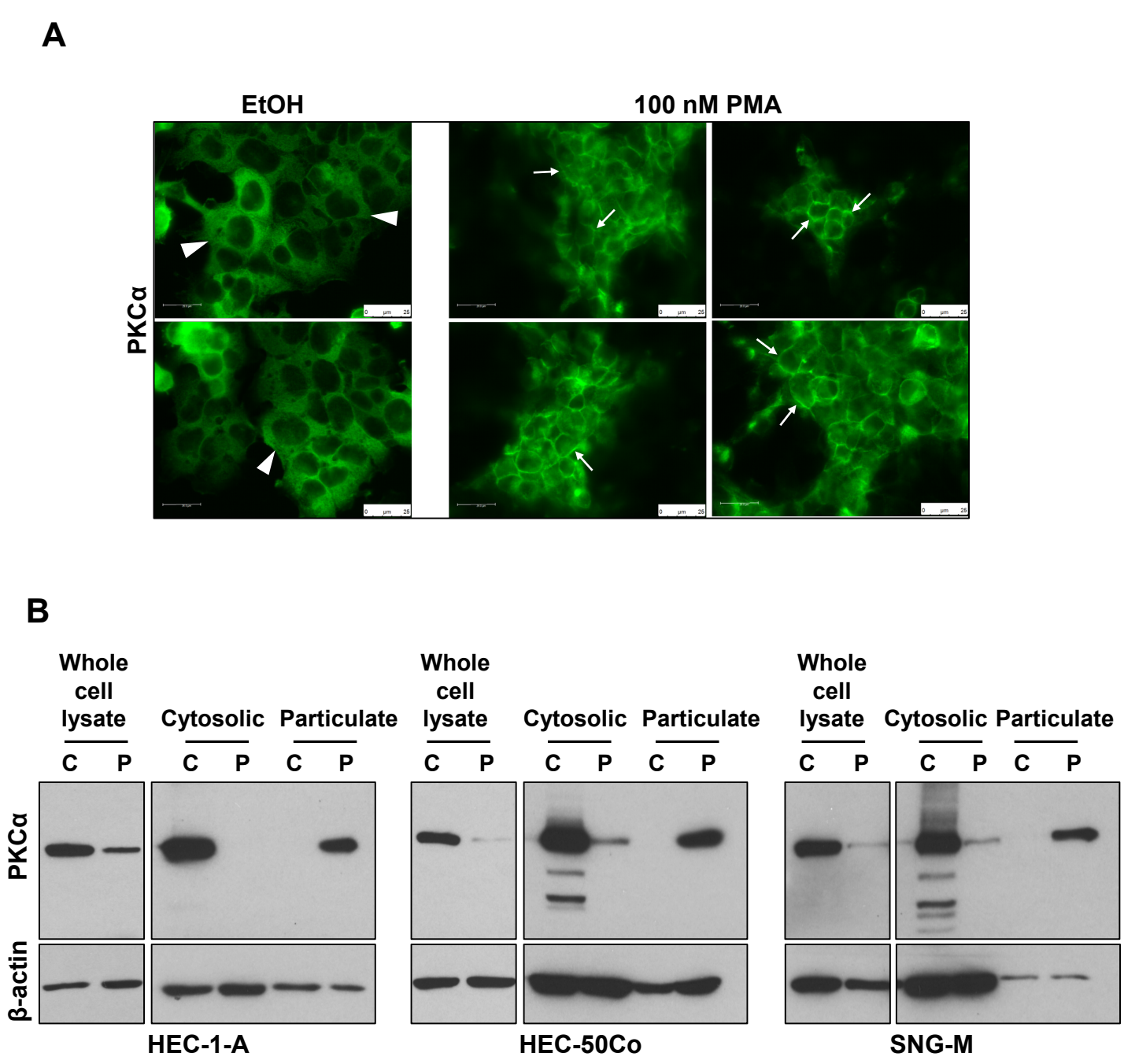

Figure S6. PKCα activation under PMA stimulation (related to Figure 5).
(A) Immunofluorescence images displaying diffuse PKCα staining in the cytoplasm at steady state (left panel) and membrane-associated PKCα (right panel), which is indicative of its activation, when endometrial cancer cells (HEC-1-A) are treated with 100 nM PMA for 6 hr. (B) Immunoblot analysis demonstrating the redistribution of PKCα from the cytosolic to the particulate fraction (right panels) following PMA-induced activation. Although total levels of PKCα are markedly downregulated after 6 hr of PMA treatment (left panels), significant levels of the enzyme persist in the particulate fraction. This level of PKCα activity is sufficient to maintain suppression of AKT activity for 6 hr (see Figure 5).

SUPPLEMENTAL TABLE

Table S1. EC cell line PI3K/AKT pathway mutations (Related to Figure 1 and Figures 3-7)

Cell line	PTEN	PIK3CA	PIK3R1
HEC-1-A	WT	G1049R	
HEC-1-B	WT	G1049R	
HEC-50Co	WT		E468InsGEYDRLYE
KLE	WT		
AN3CA	R130fs		R557_K561>Q
Ishikawa	V317fs; V290fs		L570P
RL95-2	M134I; R173H; N323fs	R386G	
SNG-II	K6fs		
SNG-M	K164fs; V290fs		R88Q
HEC-6	V85fs; V290fs	R108H; C420fs	
HEC-59	Y46H; R233X; P246L; L265fs	R38C	K567E; S460fs
HEC-108	K6fs; E288fs		A331V
HEC-116	R55_L70>S; R173C	R88Q	
HEC-151	I33del; Y76fs	C420R	
HEC-251	S10N; E299X	M1043I	
HEC-265	L318fs		H180fs; Q586fs

Adapted from (Weigelt et al., 2013).

SUPPLEMENTAL EXPERIMENTAL PROCEDURES

Human Tissue Microarrays (TMAs)

Human endometrial cancer (EC) TMAs were generated by Dr. Carl Morrison at Ohio State University (OSU) and Roswell Park Cancer Institute (RPCI) (now known as Roswell Park Comprehensive Cancer Center). Two TMAs, displaying a total of 384 de-identified ECs (304 endometrioid and 80 non-endometrioid) were generated at OSU with OSU Institutional Review Board approval. All patients in the TMA were diagnosed with uterine malignancy between January 1, 1980 and July 31, 2003 at the Arthur James Cancer Hospital of the OSU Medical School. Specimens for controls within the TMA consisted of 37 secretory endometrium, 30 proliferative endometrium, as well as multiple cores of normal tissue from 10 different organs including heart, colon, kidney, adrenal, ovary, myometrium, brain, thyroid, lung, and prostate. A third EC TMA, consisting of 52 de-identified ECs (26 endometrioid and 26 non-endometrioid) was generated at RPCI (RPCI_GYNCa09) with RPCI Institutional Review Board approval. Cases were diagnosed at RPCI between 1992 and 2011. For any case with variation in grade or cytological atypia, TMA cores of the donor block were always taken from the areas of the highest-grade tumor. Matching frozen tissue was also available for all of the RPCI cases and was used for determination of PKCα mRNA levels. Scoring of IHC staining was performed by three independent examiners who were blind to sample information.

Analysis of Publically Available Data Sets

Analysis of TCGA datasets consisting of 35 normal endometrial tissue samples and 546 primary endometrial tumors was performed using the University of Alabama at Birmingham interactive web portal (http://ualcan.path.uab.edu/analysis.html) (Chandrashekar et al., 2017). Patient survival analysis in correlation with PKCα expression was performed using the MDACC-endometrial-L3-S40 dataset, consisting of 244 endometrial tumors of which 80% were of the endometrioid subtype. Analysis of survival in relation to other PKC isozymes used both TCPA and TCGA datasets.

Cell Lines and Reagents

Human EC cell lines with diverse genetic mutations were obtained from the following sources: HEC-1-A, HEC-1-B, KLE, AN3CA, and RL95-2 from ATCC; Ishikawa from Dr. Tim Hui-Ming Huang (Ohio State University); HEC-50Co from Dr. Kimberly K. Leslie (University of Iowa); SNG-II, SNG-M, HEC-6, HEC-59, HEC-108, HEC-116, HEC-151, HEC-251, and HEC-265 cells from the Japanese Collection of Research Bioresources (JCRB) Cell Bank. All cells were maintained in culture conditions recommended by the providing source. PKC isozymes were activated with 100 nM phorbol 12-myristate 13-acetate (PMA; Biomol) dissolved in ethanol or with 20 μg/ml 1,2-dioctanoyl-*sn*-glycerol (DiC_8; Caymen Chemical) dissolved in acetonitrile. Because of its rapid metabolism in cells, DiC_8 was replaced every 30 minutes during the treatment period. Classical PKCs were inhibited with 2.5 μM Gö6976 (EMD Millipore) dissolved in ethanol. PI3K was inhibited with LY294002 (40 μM; Cell Signaling) and AKT was inhibited with MK-2206 (100 or 250 nM; Merck and Co., Inc.) dissolved in DMSO. Phosphatase inhibitors dissolved in DMSO were used as follows: calyculin A (10 nM; Santa Cruz); okadaic acid (1 μM; Santa Cruz); NSC45586 and NSC117079 (50 μM; NCI). All inhibitors were added to cells 30 minutes prior to addition of PKC agonists, except for calyculin A, which was added 15 minutes prior to PKC activation. An equal volume of vehicle was added to controls.

Stable Transfection of Cell Lines

EC cell lines stably expressing either constitutively active phosphomimetic T308D/S473D mutant AKT1 (AKT-DD) (Alessi et al., 1996) or E17K mutant AKT1 (AKT-E17K) (Carpten et al., 2007) were generated via retroviral transduction. pBMN-AKT-DD was generated by subcloning AKT-DD (BamH1/Xho1) from pEGFP-Akt-DD (a gift from Dr. Julian Downward, Addgene plasmid # 39536; Watton and Downward, 1999) into the Not1/Sal1 sites of pBMN-I-GFP (a gift from Dr. Garry Nolan, Addgene plasmid # 1736). pBabe-puro-AKT-E17K was generated by site directed mutagenesis (QuikChange) of pBabe-puro-Akt1 (a gift from Dr. X. Wang, Roswell Park Comprehensive Cancer Center, and Q. She, University of Kentucky; Fan et al., 2013) using primers CAGGTCTTGATGTACTTCCCTCGTTTGTGCAGC and GCTGCACAAACGAGGGAAGTACATCAAGACCTG. Retroviral vectors pseudotyped with VSV-G were packaged in 293GP cells and EC cells were transduced (3X) with AKT mutant or empty vector (control) in the presence of 8 μg/ml polybrene as described (Yee et al., 1994). Transduced cells were selected with 600 μg/ml G418 (pBMN-I-GFP or pBMN-I-GFP-AKT-DD) or 10ug/ml puromycin (pBabe-puro and pBabe-AKT-E17K) and stable cell lines were transduced with Ad-PKCα or LacZ and used for soft agarose colony formation assays as described below. Dr. J.C. Krapinski (McMaster University) kindly provided pLHCX-HA-CA-AKT, which was used in initial exploratory experiments that are not shown.

Mice

To generate PTEN mutant mice lacking PKCα, SV126/C57 BL6 *Prkca*$^{-/-}$ mice (Hao et al., 2011) were crossed with mixed strains of *Pten*$^{\Delta 4\text{-}5/+}$ mice (Wang et al., 2010), to generate *Prkca*$^{+/-}$; *Pten*$^{\Delta 4\text{-}5/+}$ mice. These mice were then intercrossed to generate *Prkca*$^{-/-}$; *Pten*$^{\Delta 4\text{-}5/+}$ and *Prkca*$^{+/+}$; *Pten*$^{\Delta 4\text{-}5/+}$ mice. Mouse genotypes were determined by PCR reactions using the following primers:

For *Prkca:*
Primer 1 5'-CCAAGTGTGAAGTGTGTGAG-3'
Primer 2 5'-AGCTAGGTCCTGTTGGTAAC-3'
Primer 3 5'-GCGCATCGCCTTCTTCGC-3'

For *Pten*:
CoA 5'-GAATGCCATTACCTAGTAAAGCAAGG-3'
CoB 5'-GGGTTACACTAACTAAACGAGTCC-3'
CoC 5'-GAATGATAATAGTACCTACTTCAG-3'

Immunohistochemistry

Murine uterine tissue was formalin-fixed, paraffin-embedded, and 4 μm cross- or longitudinal sections were prepared. Sections were deparaffinized in xylene and rehydrated by incubation in serially diluted alcohol. Antigen retrieval used DAKO Targeting Retrieval Solution (DAKO S1699) for 30 minutes in a steamer. Sections were blocked with 0.03% casein for 30 minutes at room temperature before incubation with primary antibody at 4°C overnight for anti-PKCα (1:3000-6000; Abcam 32376), anti-PTEN (1:100; Cell Signaling 9559), and anti-Id-1 (1:1200; Biocheck), or at room temperature for 1 h for anti-pAKT Ser473 (1:300-600; Cell Signaling 4060). Following washes, incubation with secondary antibody (Vector BA-1000) was performed at room temperature for 30 minutes, followed by washes and addition of Vectastain Elite ABC reagent (Vector Laboratories) and DAB chromogen solution (DAB Quanto; Thermo Scientific TA-060-QHDX). Sections were counterstained with hematoxylin. Immunostaining was performed using well-established IHC protocols and validated antibodies. PKCα and Id-1 were detected as described in (Hao et al., 2011), and pAKT Ser473 and PTEN IHC followed procedures detailed in (Wang et al., 2010). PKCα immunostaining specificity was further confirmed using PKCα knockout uterine tissue.

Immunofluorescence

Uterine tissue was collected and immediately frozen in OCT. Frozen sections (4-10 μm) were fixed in 2% freshly depolymerized paraformaldehyde/PBS for 15 minutes at room temperature and 100% methanol for 10 minutes at -20°C, prior to blocking with 0.03% casein and antibody incubation. Antibodies were as follows: anti-PKCα (1:250; Abcam 32376), anti-pAKT (1:200; Cell Signaling 4060), anti-rabbit Alexa 594 (1:300; Invitrogen A-21207), and anti-rabbit Alexa 488 (1:800; Invitrogen A-21206). Nuclei were stained with Hoechst dye (1:25) for 5 minutes. For analysis of PKCα localization in cell lines, $1x10^5$ cells were plated on coverslips, fixed in 2% formaldehyde and permeabilized in 100% cold methanol.

Western Blotting

Cells were rinsed twice with PBS before lysis with 1% SDS, 10 mM Tris-HCl, pH 7.4. Cell lysates were centrifuged at ≥12,000 x *g* for 20 minutes and protein concentration was determined using the BCA Assay Kit (Pierce). Equal amounts of protein were subjected to SDS-PAGE and transferred to nitrocellulose membrane. Membranes were blocked with 5% milk and probed with primary antibodies as follows: anti-PTEN (1:1000-3000; Cell Signaling 9559), anti-pAKT Ser473 (1:10,000-30,000; Cell Signaling 4060), anti-pAKT Thr308 (1:8000-20,000; Cell Signaling 2965), anti-AKT (1:1000-5000; Cell Signaling 9272), anti-pPRAS40 (1:15,000-20,000; Cell Signaling 13175), anti-PRAS40 (1:10,000; Cell Signaling 2691), anti-pFOXO1 (1:1000; Cell Signaling 9401), anti-FOXO1 (1:1000; Cell Signaling 2880), anti-PKCα (1:10,000-20,000; Abcam 32376), anti-PKCβI (1:2000; Abcam 195039), anti-PKCβII (1:1000; SC-210), anti-PKCγ (1:1000; SC-211), anti-PKCδ (1:1000; SC-213), anti-PKCε (1:1000; SC-214), anti-PKCθ (1:1000; BD trans 610084), anti-PKCη (1:500; SC-215), anti-PKCζ (1:8000; SC-216), anti-PKCι (1:1000; BD trans 610175), anti-PP2AC (1:3000; Millipore, Clone 1D6), anti-Id-1 (1:1500-3000; Biocheck), and anti-β-actin (1:15,000; Sigma). Secondary antibodies were horseradish peroxidase-conjugated anti-rabbit or anti-mouse IgG (1:2000) and detection used SuperSignal West (Pierce). Signal intensity was quantified using ImageJ Software (NIH).

qRT-PCR Analysis
RNA was isolated using RNAspin mini RNA isolation kit (GE Health) or Trizol reagent (Thermo Fisher) and 10 ng total cellular RNA was analyzed using Brilliant II SYBR® Green QRT-PCR 1-Step Master Mix (Agilent). The primers used for each target were as follows.

PKCα: 5'-GGAAGGGGACGAGGAAGGA-3', 5'-TGATGACTTTGTTGCCAGCAG-3';
PHLPP1: 5'-TGATGACTTTGTTGCCAGCAG-3', 5'-AGTTCATTAAGCCCCCTGGC-3';
PHLPP2: 5'-TGTACGCAAGGGAAAGACCC-3', 5'-AGCAAGGGAGTATTGCCGTC-3';
18s rRNA: 5'-CATTGGAGGGCAAGTCTGGTG-3', 5'- CTCCCAAGCTCCAACTACGAG-3';
GAPDH: 5'-TGAAGGTCGGAGTCAACGGA-3', 5'-CCATTGATGACAAGCTTCCCG-3'

Laser Capture Microdissection (LCM)
Longitudinal sections (10 μM) of frozen tissue (in OCT compound) were thaw-mounted onto PET-membrane FrameSlides (Leica). Slides were air-dried briefly and fixed in 70% EtOH for 30 seconds, washed in dH_2O to remove excess OCT, stained with hematoxylin until tissue was visible, rinsed in dH_2O, and incubated in 95% and 100% EtOH for 30 seconds. LCM was performed using a Leica LMD 6500 Laser Microdissection System. Collection of normal endometrial epithelium and hyperplastic lesions was guided by immunofluorescence analysis of PKCα and pAKT Ser473 expression on adjacent sections. Microdissected tissue was directly collected into lysis buffer and RNA was isolated using the RNAqueous-MicroKit (Ambion).

Subcellular Fractionation
Cytosolic and particulate fractions were prepared from endometrial cancer cells and an equal proportion of each fraction was analyzed for PKCα expression as described (Frey et al., 1997).

Correlation between PKCα mRNA and Protein Levels in EC Tissues and Cell Lines
To perform parallel analysis of PKCα mRNA and protein levels in EC tumors, total RNA was isolated from frozen samples of 52 of the tumors included in the TMA. PKCα mRNA levels were measured by qRT-PCR. A score was given to the tumors based on PKCα signal intensity from the IHC analysis. Results from the mRNA analysis were paired with the corresponding IHC score for the 52 tumors. The correlation between PKCα mRNA and protein levels was determined by Spearman Rank Correlation analysis.

Quantification of Tumor Burden and pAKT Intensity Relative to PKCα Expression
For quantification of uterine tumor burden in mice, two to four longitudinal sections per animal were stained for pAKT Ser473 to identify endometrial lesions (Wang et al., 2002) and positive signal was quantified using DEFINIENS software and expressed relative to total endometrial epithelium area (as %).

For determination of pAKT intensity relative to PKCα expression, pAKT staining on each slide was stratified as negative-low, medium and high without knowledge of corresponding PKCα staining. Analysis was performed using Adobe Photoshop CC. pAKT staining was abstracted from the image using the Color Range tool and copied to a separate layer. Thresholds corresponding to the boundaries between staining levels were set and used to trace areas corresponding to each level. Areas of positivity on slides probed for PKCα were similarly identified and abstracted to a separate layer without reference to pAKT staining. Layers from consecutive slides stained for PKCα and pAKT were overlaid and the area (in pixels) corresponding to each level of pAKT staining in PKCα positive and PKCα negative areas was determined.

Analysis of Nascent RNA
Labeling and capture of nascent RNA were performed using the Click-iT Nascent RNA Capture Kit (Life Technologies) according to the manufacturer's protocol. Biotinylated RNA was captured using Streptavidin magnetic beads and cDNA was generated using the iScript cDNA Synthesis Kit (Bio-Rad). cDNA for PKCα and GAPDH was quantified by qPCR using iTaq Universal SYBR Green Supermix.

RNA Interference
Lentiviral transduction of cells with PTEN shRNA (clones V2LHS_92317 and/or V2LHS_231477; Open Biosystems) or a non-targeting (nt) shRNA (RHS4348) was at a multiplicity of infection (moi) of 20 in serum-free medium containing 8 μg/ml of polybrene. Cells were incubated with lentivirus for 8 hours at 37°C before the addition of serum-containing culture medium. Four days after transduction, cells were continuously selected with puromycin (10 μg/ml)

prior to use in experiments. For siRNA-mediated knockdown of PKCα, cells were transfected with 10 nM siRNA using RNAiMAX transfection reagent (Invitrogen) and analyzed after 48-72 h. siRNAs were as follows: PKCα siRNA 1 – 5'-GGAUUGUUCUUUCUUCAUATT-3' (Ambion Life Technologies); PKCα siRNA 2 – 5'-GAAGGGUUCUCGUAUGUCATT-3' (Ambion Life Technologies); Non-targeting siRNA #1 D-001810-01-05 (Dharmacon).

PP2A Activity Assay

Cells were treated with PMA or vehicle control for 10 minutes and PP2A activity in cell extracts was measured using a PP2A Immunoprecipitation Phosphatase Assay Kit (Millipore) as previously described (Guan et al., 2007), except that 0.5% Ipegal CA-630 was included in the lysis buffer.

Adenoviral-mediated Protein Expression and Soft Agarose Colony Formation Assay

Adenoviral vectors expressing either LacZ (control), PKCα, or kinase-dead PKCα were amplified in HEK293 packaging cells and the titer of viral supernatants was determined using Adeno-X Rapid Titer Kit (Clonetech). Adenovirus expressing myr-AKT1 or PTEN was purchased from Vector Biolabs. Cells (5×10^5) were transduced with adenovirus in reduced (2%) serum medium for 24 hours and then incubated in complete culture medium for 24 h prior to drug treatment and Western blot analysis as described in previous sections. Alternatively, $1\text{-}5\times10^3$ cells per well were plated in 0.6% low-melting agarose in duplicate as described (Pysz et al., 2009). Ad-LacZ was used as a control for adenoviral protein expression. Colonies were allowed to grow for 1-4 weeks prior to staining with crystal violet. Whole plates were then scanned and visible colonies were counted. Alternatively, images from 4 independent fields per well were taken at 5X magnification at 4 different focal planes. Images of colonies from each focal plane were selected and superimposed using the magic wand tool in Adobe Photoshop CC software. The number of colonies per field was determined using the Particle Analysis Tool in Image J Software (NIH).

SUPPLEMENTAL REFERENCES

Alessi, D.R., Andjelkovic, M., Caudwell, B., Cron, P., Morrice, N., Cohen, P., and Hemmings, B.A. (1996). Mechanism of activation of protein kinase B by insulin and IGF-1. The EMBO Journal *15*, 6541-6551.

Byers, S.L., Wiles, M.V., Dunn, S.L., and Taft, R.A. (2012). Mouse estrous cycle identification tool and images. PLoS One *7*, e35538.

Carpten, J.D., Faber, A.L., Horn, C., Donoho, G.P., Briggs, S.L., Robbins, C.M., Hostetter, G., Boguslawski, S., Moses, T.Y., Savage, S.*, et al.* (2007). A transforming mutation in the pleckstrin homology domain of AKT1 in cancer. Nature *448*, 439.

Chandrashekar, D.S., Bashel, B., Balasubramanya, S.A.H., Creighton, C.J., Ponce-Rodriguez, I., Chakravarthi, B.V.S.K., and Varambally, S. (2017). UALCAN: A Portal for Facilitating Tumor Subgroup Gene Expression and Survival Analyses. Neoplasia *19*, 649-658.

Daikoku, T., Hirota, Y., Tranguch, S., Joshi, A.R., DeMayo, F.J., Lydon, J.P., Ellenson, L.H., and Dey, S.K. (2008). Conditional loss of uterine Pten unfailingly and rapidly induces endometrial cancer in mice. Cancer Res. *68*, 5619-5627.

Daikoku, T., Ogawa, Y., Terakawa, J., Ogawa, A., DeFalco, T., and Dey, S.K. (2014). Lactoferrin-iCre: A New Mouse Line to Study Uterine Epithelial Gene Function. Endocrinology *155*, 2718-2724.

Fan, C.-D., Lum, M.A., Xu, C., Black, J.D., and Wang, X. (2013). Ubiquitin-dependent Regulation of Phospho-AKT Dynamics by the Ubiquitin E3 Ligase, NEDD4-1, in the Insulin-like Growth Factor-1 Response. J. Biol. Chem. *288*, 1674-1684.

Frey, M.R., Saxon, M.L., Zhao, X., Rollins, A., Evans, S.S., and Black, J.D. (1997). Protein kinase C isozyme-mediated cell cycle arrest involves induction of p21(waf1/cip1) and p27(kip1) and hypophosphorylation of the retinoblastoma protein in intestinal epithelial cells. J. Biol. Chem. *272*, 9424-9435.

Guan, L., Song, K., Pysz, M.A., Curry, K.J., Hizli, A.A., Danielpour, D., Black, A.R., and Black, J.D. (2007). Protein kinase C-mediated down-regulation of cyclin D1 involves activation of the translational repressor 4E-BP1 via a phosphoinositide 3-kinase/Akt-independent, protein phosphatase 2A-dependent mechanism in intestinal epithelial cells. J. Biol. Chem. *282*, 14213-14225.

Hao, F., Pysz, M.A., Curry, K.J., Haas, K.N., Seedhouse, S.J., Black, A.R., and Black, J.D. (2011). Protein kinase Calpha signaling regulates inhibitor of DNA binding 1 in the intestinal epithelium. J. Biol. Chem. *286*, 18104-18117.

Pysz, M.A., Leontieva, O.V., Bateman, N.W., Uronis, J.M., Curry, K.J., Threadgill, D.W., Janssen, K.P., Robine, S., Velcich, A., Augenlicht, L.H., *et al.* (2009). PKCalpha tumor suppression in the intestine is associated with transcriptional and translational inhibition of cyclin D1. Exp. Cell. Res. *315*, 1415-1428.

Wang, H., Douglas, W., Lia, M., Edelmann, W., Kucherlapati, R., Podsypanina, K., Parsons, R., and Ellenson, L.H. (2002). DNA mismatch repair deficiency accelerates endometrial tumorigenesis in Pten heterozygous mice. Am. J. Pathol. *160*, 1481-1486.

Wang, H., Karikomi, M., Naidu, S., Rajmohan, R., Caserta, E., Chen, H.Z., Rawahneh, M., Moffitt, J., Stephens, J.A., Fernandez, S.A., *et al.* (2010). Allele-specific tumor spectrum in pten knockin mice. Proc. Natl. Acad. Sci. USA. *107*, 5142-5147.

Watton, S.J., and Downward, J. (1999). Akt/PKB localisation and 3' phosphoinositide generation at sites of epithelial cell-matrix and cell-cell interaction. Current biology : CB *9*, 433-436.

Weigelt, B., Warne, P.H., Lambros, M.B., Reis-Filho, J.S., and Downward, J. (2013). PI3K pathway dependencies in endometrioid endometrial cancer cell lines. Clin. Cancer. Res. *19*, 3533-3544.

Yee, J.K., Miyanohara, A., LaPorte, P., Bouic, K., Burns, J.C., and Friedmann, T. (1994). A general method for the generation of high-titer, pantropic retroviral vectors: highly efficient infection of primary hepatocytes. Proc Natl Acad Sci U S A *91*, 9564-9568.